IMPROVED IN-ROAD SENSING DEVICE FOR PAVEMENT HEALTH MONITORING USING IOT

I RICHARDS, AJ HOFFMAN, L KLOPPERS and J VISAGIE

School of Electrical, Electronic and Computer Engineering, North-West University,
Private Bag X6001, Potchefstroom 2520, South Africa

ABSTRACT

Continuous pavement health monitoring enables the detection of early degradation of pavement structures, thereby extending the lifetime of roads by informing predictive maintenance actions. A previous paper described a method that enables low cost, high coverage, and continuous monitoring of the displacement, temperature, humidity and moisture content of pavement structures. The pavement condition outcomes are communicated to a hub using a LoRa sensor network that combines long read range, low power consumption and sufficient communication speed, while a solar cell and battery provide continuous power to allow 24/7 operation even in dense traffic conditions. This paper reports on the development and evaluation of an improved version of this system. The number of accelerometers was increased from one to four to allow assessment of pavement condition at different depths below the surface. The on-board software was extended to allow the capturing of measurements to be automatically triggered either by a magnetometer, that senses the presence of large metal objects, or by using the acceleration signal itself, implementing a sliding window to prevent the loss of data captured before the trigger threshold is exceeded. The displacements derived from acceleration measurements were compared against LVDT-based displacement measurements and found to be accurate within a few percent. The LoRa sensor network allows the real-time communication of selected features like peak signal amplitude, as well as the communication of detailed measurements during quiet times to allow the impact of heavy vehicles to be characterised in detail.

1. INTRODUCTION

Road infrastructure plays a critical role in supporting safe and efficient transportation systems. However, road degradation poses significant challenges, as heavy traffic, frequent use by large vehicles, and wet weather conditions contribute to the formation of cracks in the road pavement. Combined with inadequate road maintenance, this has resulted in numerous unsafe roads characterized by uneven surfaces and potholes (Kgamanyane & Hartzenberg, 2015).

Potholes primarily form due to the presence of water, although their development varies based on the road structure, materials, and construction quality. As vehicles pass, they cause the road to deflect, and repeated high deflections, especially from overloaded vehicles, contribute to crack formation (Alrajhi et al., 2023). Small surface cracks in the pavement allow water to penetrate the inner structure, leading to deterioration at deeper levels. Ultimately, the combination of wet conditions and heavy road deflections leads to large pothole formation, and eventually the complete degradation of the road, such as the one shown in Figure 1. These conditions not only make driving uncomfortable but also increase the risk of accidents.

Currently, identifying potholes and uneven surfaces typically relies on visible detection at the surface. Unfortunately, visible signs of deterioration usually indicate that extensive damage has already occurred within the road structure. This delay in detection not only complicates repair processes but also increases the costs associated with road maintenance. The ability to identify early signs of road damage could allow for more cost-effective maintenance strategies. Existing techniques to repair early signs of road damage include crack sealing and resurfacing (Alrajhi et al., 2023).

Figure 1: Formation of potholes on road (Alrajhi et al., 2023)

1.1 Aim of Paper

This paper builds on previous work (Fiorita et al., 2023) and focuses on the development of an improved smart in-road sensor (SIRS) device designed for continuous monitoring of pavement behaviour under dynamic loading and real-world conditions without disrupting traffic. The SIRS is embedded within the road infrastructure and equipped with sensors to measure critical parameters, including temperature, humidity, vibrations, and deflections caused by passing vehicles. By continuously gathering and analyzing this data, the SIRS provides valuable insights into the condition of the road, which will allow the detection of early road degradation. The improved device reduces the size of the hole to be drilled in the road pavement, increases the number of sensors to allow measurements at different depths, implements onboard extraction of signal features to reduce the required volume of wireless data communication, and packages the data in a suitable format to be used by the wireless sensor network.

1.2 Problem Statement

The literature research indicates that road owners and custodians need a monitoring solution that can measure the impact of individual vehicles on road pavements and identify early-stage road degradation in real time. The deployment of such a solution will result in more timely and cost-effective repairs to roads, thus preventing serious road degradation and the eventual complete destruction of the road.

1.3 Scope of Paper

The paper will detail the design of the improved in-road sensor device, and its testing in different scenarios. It involves redesigning the electronics and packaging to fit a hole drilled by a standard 100 mm diameter drill bit (compared to the 150 mm diameter of the previous design), increasing the number of each type of sensor (accelerometer, humidity and temperature) to 4 to allow the pavement condition to be measured at different depths below the road surface, converting the acceleration signals to displacement and extracting

maximum displacement amplitudes on the onboard processor to reduce the volume of data to be communicated, packaging the data to optimally utilize the LoRaWAN protocol, and enabling wireless configuration of the device to support remote device management, as would be required for a large deployment of such devices across a national road network. The proposed concept is illustrated in Figure 2.

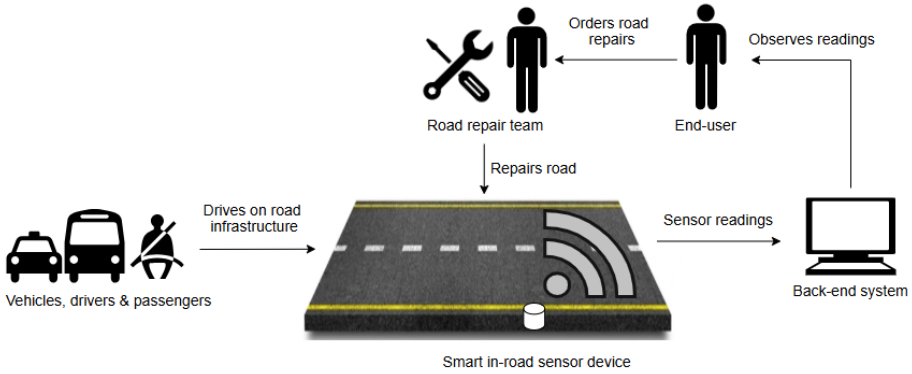

Figure 2: Diagram showing the system solution on a high-level

2. LITERATURE STUDY

When a stress or load such as the wheel of a vehicle moves over a road, the road will undergo displacement in all directions. The magnitude of the vertical displacement is however the most significant. The Falling Weight Deflectometer (FWD) Method is a popular non-destructive test that is used to determine how much a pavement surface bends or deflects when a known load is applied (Kavussi et al., 2017). Deflection data obtained from an FWD can be used to generate a profile called a deflection basin, which shows how the pavement deflects at the point of contact as well as the surrounding areas. The largest deflection occurs near the loading center, and decreases as the distance from the centre increases (Kavussi et al., 2017).

In another paper (Natasha et al., 2020) the authors found that typical road deflection levels are between 0.1 mm and 1 mm. The deflection profile that a road undergoes when a 5-axle semi-trailer vehicle weighing 40 tons pass over it is displayed in Figure 3. From the diagram, five downward peaks can be observed, which correspond to the five axles of the vehicle. The amplitude of the deflection is dependent on the axle loads as well as the speed at which the vehicle travels. It can also be observed that when axles are closely spaced, such as the three at the back of a truck, the road does not have sufficient time to return to its resting position. Consequently, the road moves back down almost immediately after beginning to rise back up. Similar results are found in another paper (Arraigada et al., 2009) in which the authors investigates road deflections using an accelerometer and deflectometer.

Acoustic sensors have also been suggested to measure the condition of roads. Vehicles driving over the road generate noise and vibrations which then travel through the road in the form of acoustic signals. In (Rosario et al., 2017) the spectral content of acoustic signals generated by the road pavement under vehicular traffic conditions was analysed, based on the idea that the spectral content of a received acoustic signal travelling through an uncracked slab is different from the spectral content of an acoustic signal received travelling through a cracked slab.. A prototype was developed and tested in a lab by inserting a microphone into a small hole of both a cracked and uncracked slab of asphalt. A Wheel Tracking Machine (WTM) was used as a source for vibrations and sound. A similar method using acoustic signatures (Cafiso et al., 2021) mounts the acoustic sensor

unit on the road surface. An advantage of this method was that the testing could be carried out in a non-destructive way. A Light Weight Deflectometer (LWD) was used to produce sound and vibrations to test the system.

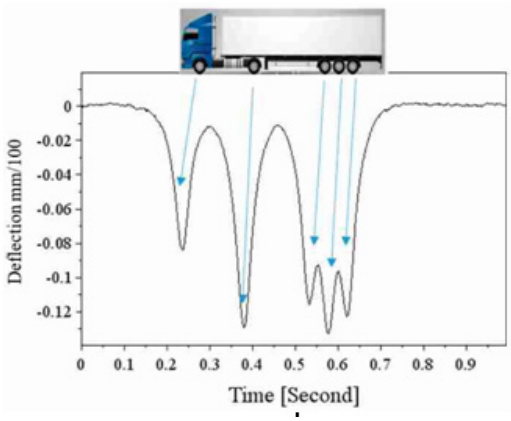

Figure 3: Road deflection caused by a 5-axle truck

The use of MEMS accelerometers has become a popular method for road condition monitoring. In (Bajwa et al., 2020) the authors developed a cost-effective small wireless accelerometer system similar to the SIRS. The device consists of three main parts: vibration sensors (accelerometers), vehicle detection sensors, and an access point. Both the vehicle detection sensors and accelerometers are placed within the road infrastructure and the rest of the equipment is located on the side of the road. To use the accelerometers to estimate the road displacement, the accelerometer should have a resolution of 500 µg (1 g=9.81 m / s2), a bandwidth of 50 Hz, and a range of ± 200 mg (Alrajhi et al. 2023). A sampling frequency of 512 Hz was used for the accelerometer. As the accelerometers are highly sensitive to highway noise, the use of a sensor casing and a low pass filter to reduce the noise was recommended. A 3rd-order Butterworth low pass filter with a cut-off frequency of 50 Hz was used to eliminate the noise.

In another paper (Ye et al.), a MEMS accelerometer was used with a sampling rate of 1 kHz to capture vibrations, process them, and transmit them to a back-end system. The use of accelerometers however produces a large amount of raw data, which is a challenge for transmission in Wireless Sensor Networks (WSNs) as they have limited bandwidth. If the communication module is on for longer periods, more power is used. To address this problem, the paper recommends the use of pre-processing techniques and algorithms to improve signal quality and remove redundant data. These techniques include feature extraction, baseline correction, filtering and smoothing, and threshold setting.

To obtain a displacement signal from an acceleration signal (Bajwa et al., 2020) propose three different methods. The first method involves using the fundamental mathematical relationship between displacement, velocity, and acceleration. The position signal of a body can be calculated by integrating the acceleration signal twice. This method can lead to unexpected drift in the estimated displacement signal due to the integration operation disproportionally amplifying measurement errors at low frequencies. Even a tiny offset in the acceleration signal can cause the resulting displacement signal to drift significantly. This is shown with the blue trace in Figure 4, where the road is initially seen to have a displacement of 0 µm. After the road undergoes a displacement reaching 70 µm, it starts to go back to its initial position. However, in the end, the road is seen to have a resulting calculated displacement of 50 µm, and not 0 µm. A possible correction technique to remove the drift from such a signal. It involves fitting a polynomial to the signal and then subtracting the polynomial from that signal. The second method to obtain displacement

from acceleration is to make use of a Constrained Least-Squares Estimation algorithm. The third method is Model-based estimation, which involves approximating the response of the pavement using a family of functions. The use of a Kalman filter has also been proposed as an alternative correction technique (Ferrero et al., 2016).

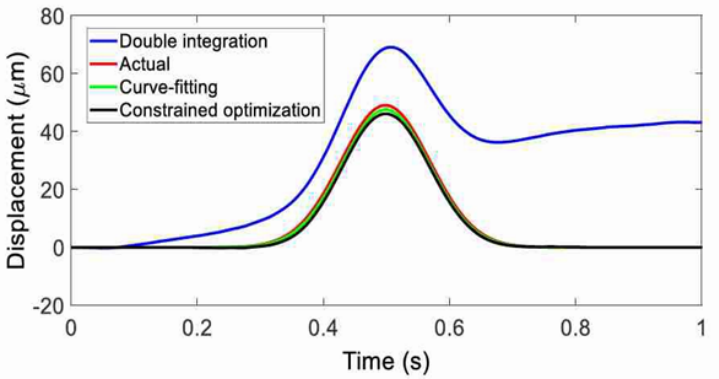

Figure 4: Example of drift because of double integration

3. SIRS DESIGN

3.1 System Architecture

Based on the literature research and taking into consideration the problem statement, a proposed solution is provided in Figure 5. The architecture diagram provides a high-level view of the entire system, showing the main entities involved as well as their interfaces with one another. The primary focus of this paper will be on the design and implementation of Functional Unit 1.0 (the SIRS).

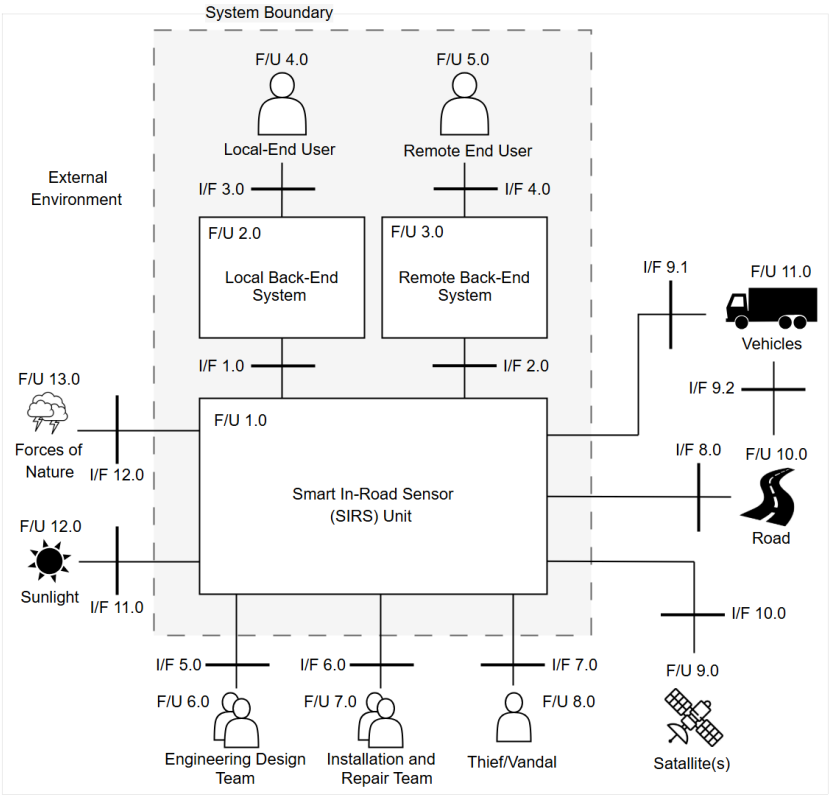

Figure 5: Architecture diagram showing the SIRS on a concept level

Table 1 provides a description of the functional units and interfaces in Figure 5.

Table 1: Description of the functional units shown in Figure 5

F/U	Name	Description
1.0	Smart in-road sensor unit	This is the device that will be installed into the road infrastructure. It contains among other things: sensors, a power supply unit with solar panel, a microprocessor, non-volatile memory, wireless communication modules, and a control unit. A casing encloses these components.
2.0	Local back-end system	This back-end system located within 5 m of the SIRS is used for on-site testing during the installation stage by technicians for quick verification of the SIRS's functionality. It consists of a laptop that receives data transmitted by the SIRS and visually displays it on the laptop screen and/or save the data as CSV files.
3.0	Remote back-end system	A permanent back-end system which is located further away from the SIRS and that communicates with it via LoRaWAN and the Internet. This back-end system receives and stores the data transmitted by the SIRS during operational mode. The back-end system is scaled to the size of the deployed networks of SIRS devices.
4.0	Local end-user	The results received and displayed by the local back-end system are presented to an end-user on-site. This may be a technician responsible for installation or maintenance of the SIRS network.
5.0	Remote end-user	This may be a road maintenance technician who uses the captured results to infer the condition of the road.
6.0	Engineering design team	A team responsible for the design and implementation of the SIRS who may be present during the installation stages of the SIRS if needed.
7.0	Installation and repair team	A qualified and trained team of technicians is responsible for installing and activating the SIRS as well as attending to any future repairs and updates. The installation process includes the drilling of the core hole in the road, the installation of the SIRS package inside the hole, and verifying the functionality of the SIRS.
8.0	Thief/Vandal	As the SIRS is installed inside the road, which is a public space, it may be subjected to theft or vandalism.
9.0	Satellite(s)	The GNNS module inside the SIRS rely on communication with GNNS satellites. This module is used both for time synchronization as well as to inform the user of the installed location of the SIRS, in case this information is not captured correctly during installation.
10.0	Road	The physical infrastructure into which the SIRS will be embedded and on which vehicles drive. Road pavements usually consist of multiple layers, although the number of layers as well as the thickness varies from one road to another.
11.0	Vehicles	Vehicles driving on the road surface place a force on the layers beneath. The vibrations and displacement caused by vehicles lead to road damage and the eventual formation of potholes.
12.0	Sunlight	As the SIRS makes use of solar power energy as its power source, sunlight is required to shine on the solar panel for the generation of a DC voltage.
13.0	Forces of nature	Weather conditions and earthquakes can cause damage to the sensitive electronic components inside the SIRS which may impact its performance. This can lead to inaccurate data capture from the sensors, failure to transmit the results to the back-end system, and worst-case lead to the complete failure and damage of the SIRS.

3.2 Component Selection

The following criteria were taken into consideration for the selection of the most suitable components:

1. 3.3 V power supply
2. Low power consumption
3. Maximum CPU clock speed no lower than 60MHz
4. Ideally 512kB Flash
5. Ideally 128kB SRAM or higher
6. 4x UART channels
7. 4x I2C channels
8. 3x SPI channels
9. Enough additional GPIO pins
10. A DSP unit
11. Interface with host MCU via UART, I2C, or SPI
12. Acceleration range should be ±2g.
13. Short range communication at least 5 m range and data rate ≥ 100 kbps
14. Long range communication at least 1 km range and data rate ≥ 10 kbps
15. Bandwidth not less than 50Hz
16. ODR not less than 1kHz
17. Noise level as low as possible
18. Physical size as small as possible
19. Price as low as possible

The table below describes the components that were selected based on these criteria.

Table 2: Components selected for SIRS

Component Type	Selected Component
Microcontroller Unit	STM32L451RE
Short-Range Communication Module	Microchip RN4871-I/RM130 wireless Bluetooth module
Long Range Communication Module	453-00140R LoRa module
Location Transceiver Module	UBLOX SAM-M10Q GNNS module
Temperature and Humidity Sensors	Texas Instruments HDC3022 temperature and humidity sensor IC
Accelerometers	Rohm Semiconductor KX132-1211 accelerometer
Magnetometer	ST Electronics LIS3MDL
Non-volatile Storage Device	Micro-SD card
User Feedback Unit	LEDs

Figure 6 shows the PCB layout while Figure 7 shows the fully assembled main SIRS PCB.

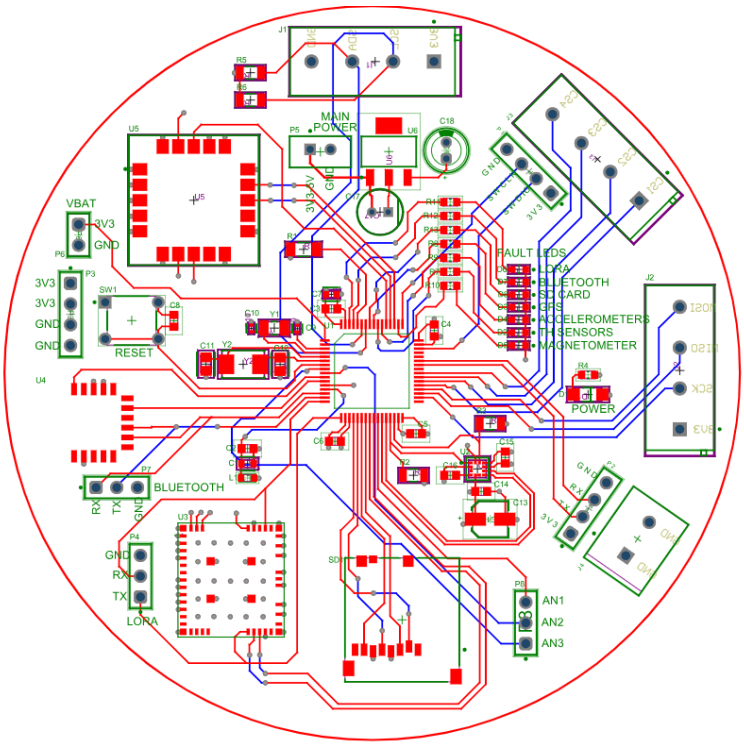

Figure 6: SIRS PCB layout

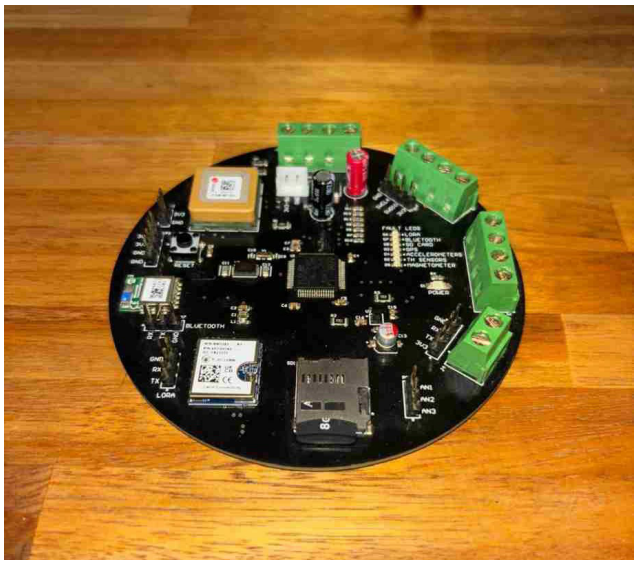

Figure 7: SIRS board fully assembled

3.3 Power Budget

The same solar panel as used for previously reported work (Fiorita et al., 2023) is employed. The panel has a size of 55x70 mm with a maximum output of 550 W, which produces a generation capability of approximately 2000 mWh for an autumn day. It is important to note that not all peripherals will function continuously. The temperature and humidity sensors will only collect measurements every 15 minutes to an hour and the GNNS coordinates will only be determined on startup. Only the accelerometers will always remain active. In normal operations the Bluetooth module will not be active. This leaves only the MCU itself, the LoRa module and the accelerometers to consume power under normal operating conditions. Table 3 displays the calculations for the expected power consumption of the in-road sensor.

Table 3: Power budget for in road sensor

Components	Quantity	Component Current Consumption (mA)	Total Cosumption (mA)	
Accelerometers [1]	4	0.152	0.608	
Temperature Sensors [2]	4	0.021	0.083	
MCU [3]	1	13.490	13.49	
LORA [4]	1	2.853	2.8531	
		Total	17.0344	
		Total Power (@3.3V)	56.2136	mW
		Total Power day	1349.1264	mWh

Power Generation and storage	Generation Capability per day	
Solar Panel (55* 70mm)	2	Wh (approx as measured)
Battery (5000 mAh @3.7 V)	18.5	Wh

Without charging till flat	13.713	days
Time till full Charge if battery is flat and system is running	12.041	days

1) output data rate of 800 Hz
2) Temperature sensors will only be active once an hour
3) operating at max clock speed of 80 MHz
4) assuming send and receive direclty after one another with a payload of 115 bytes over SF 9

From these calculations it can be seen that the expected battery lifetime for the device is nearly two weeks with no solar input and that it will also take nearly two weeks for the battery to fully recharge if the battery is in a depleted state. It should also be noted that the generation capability will vary across seasons (higher during summer and lower during winter), potentially differing by up to 30%.

3.4 Packaging

Protection of the SIRS and its components requires suitable enclosures. The accelerometers enclosures allow the sensor PCB to be tightened inside the enclosure using a screw cap. The 3D printed accelerometer enclosure is shown in Figure 8. The sensor wires which exit the enclosures at the bottom were then spliced and connected to the accelerometers terminal block on the main SIRS PCB. Figure 9 shows the fully assembled system, consisting of all sensors and PSU connected to the main SIRS PCB.

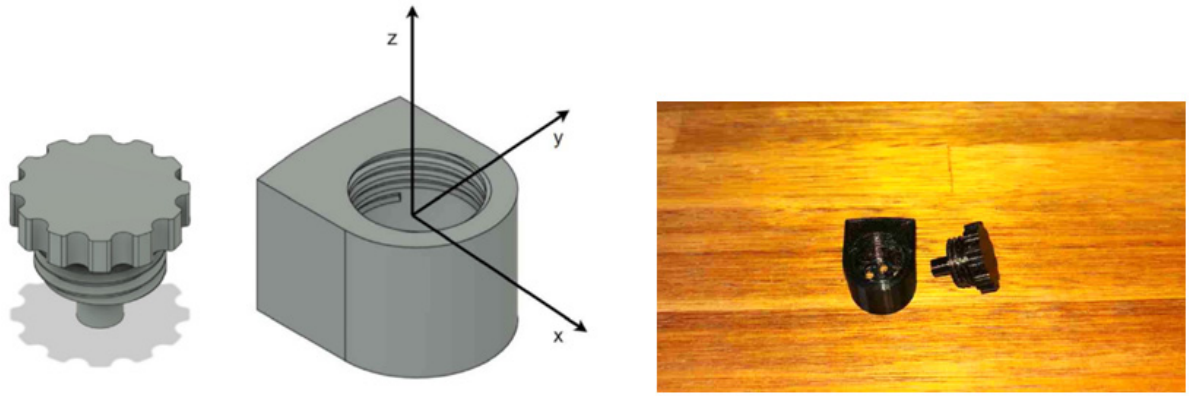

Figure 8: 3D printed accelerometer enclosure

As the temperature and humidity sensors must measure the temperature and humidity inside the road infrastructure at different levels, the face of the sensor IC must be exposed to the interior environment of the road to allow the condition of the road to be accurately captured. A conformal coating is applied to the sensor PCBs, exposing only the top of the sensor IC. The installation approach entails making a small hole in the road pavement, at

the appropriate depth inside the main cavity, and placing the sensor PCB with its conformal coating inside the hole. This small opening will be exposed to the actual temperature and humidity inside the road. After the sensors are placed into the holes, the opening is closed using an appropriate sealant such as putty to maintain the integrity of the measurements. Figure 6 shows the installation concept. Note that the diagram is not drawn according to scale and that the rest of the SIRS is omitted.

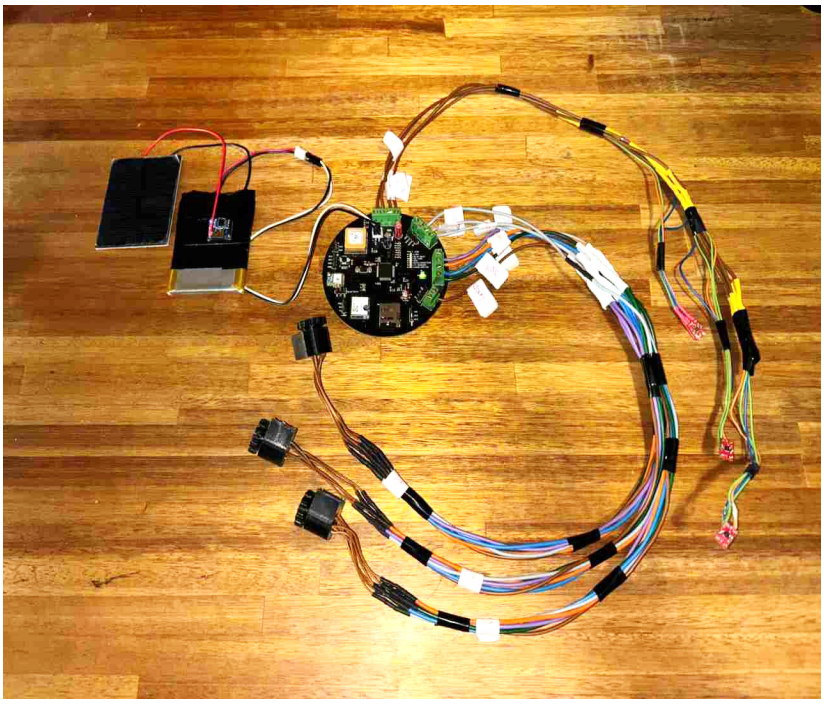

Figure 9: SIRS fully assembled

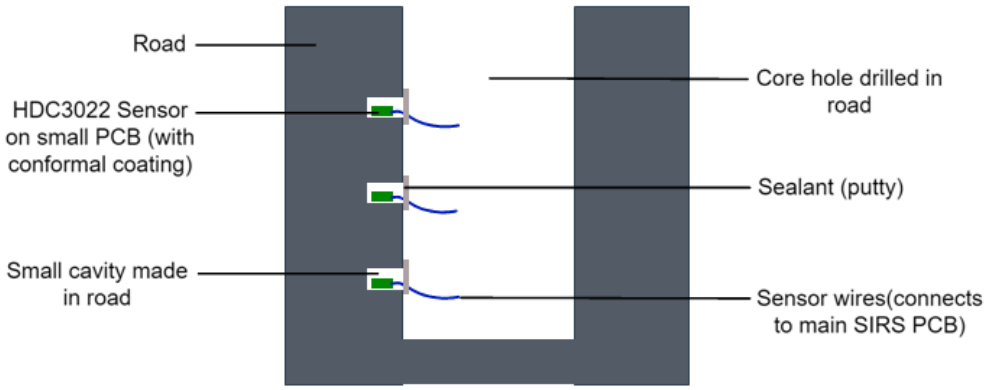

Figure 10: Diagram showing the method for placing temperature and humidity sensors inside the road infrastructure

4. RESULTS

4.1 Laboratory Tests

Accelerometer Performance Test

Purpose:

The purpose of this test is to evaluate how effectively the KX132-1211 accelerometer measures acceleration in a controlled environment, and to determine whether corres-

ponding displacement signals can be derived from the captured acceleration signals. The accelerometer was mounted on a MTS Landmark Servo hydraulic test system that generates controlled movements of which the shape, amplitude and frequency can be set (Natasha, Juliette et al. 2020).

Method:

1. Set the machine to move the platform in a sinusoidal motion with a peak-to-peak amplitude of 0.2 mm and a frequency of 5 Hz.
2. Begin sampling the accelerometers just before starting the machine. This ensures that zero conditions are met, which is crucial for the subsequent integration operation.
3. Use the SD card to transfer the file to a laptop and import the captured signal into a Python script.
4. Remove the DC offset present in the acceleration signal to eliminate drift during integration.
5. Perform double integration on the accelerometer signal to obtain the position signal.
6. Apply a 2nd order Butterworth bandpass filter to remove the dominant low-frequency component and any noise from higher frequencies.
7. Compare the corrected position signal with the expected movement set by the machine.
8. Repeat steps 1-7 for frequencies 10, 15, and 20Hz.

Figure 11: Accelerometer and LVDT set up in lab showing the LVDT and accelerometer mounted to the machine. (LVDT mounted in blue pipe, Accelerometer circled in red)

Results:

For brevity only the results for the 10 Hz signal is displayed in Figure 12. The green signal on the top graph represents the captured acceleration signal when the machine is set to move with a peak-to-peak amplitude of 0.2 mm. With regards to the second graph the red signal represents the LVDT output, and the green signal shows the displacement after the position signal has been processed through the bandpass filter. The final graph shows the output as obtained from the machine itself. An upper cut-off frequency of 12 Hz and a lower cut-off frequency of 8 Hz were found to provide the best results. Similar results were obtained at the other frequencies.

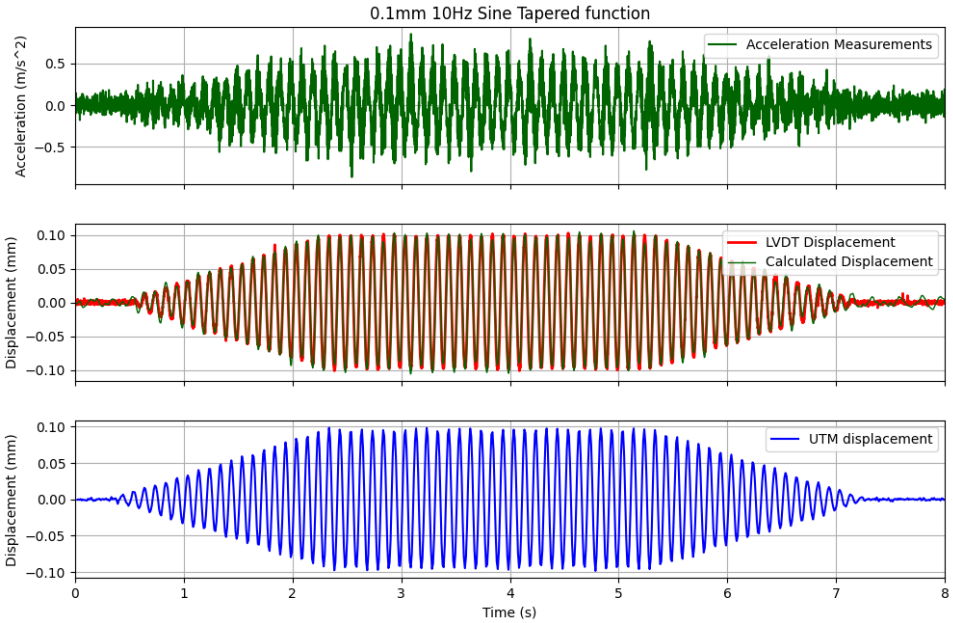

Figure 12: Vibrational test for 10Hz signal

Discussion:

The peak-to-peak amplitude of 0.2 mm was specifically chosen because it closely reflects the amplitude that roads experience when vehicles traverse them (Arraigada, Partl et al., 2009). The measured results demonstrated that the displacements extracted from the measured accelerometer signals effectively captures the displacements caused by the machine's vertical movement. The resulting position signals exhibit sinusoidal shapes, with the signals achieving nearly perfect steady sinusoidal amplitudes of ±0.1 mm (or 0.2 mm peak-to-peak). The frequencies of the signals were verified using FFT analysis, confirming that they matched the set frequency of the machine's reference signal.

4.2 In-Road Tests

The second set of tests were conducted to evaluate the performance of the temperature, humidity and accelerometers and the effectiveness of the acceleration to displacement algorithm in a practical in-road setting. These tests were performed at core holes located on the NWU campus that were drilled to fit the SIRS packaging. Figure 13 (a) and (b) display the sensors and the complete SIRS device installed into the core hole on NWU campus and on the N4, respectively. The external antenna of the LoRa unit can be seen next to the solar panel. The GNSS module has an internal (built-in) antenna, thus no external antenna can be seen.

The first in-road test was aimed at capturing temperature and humidity levels inside the road on three different layers over a 12-hour period. These measurements were taken at depths of 50mm, 100mm, and 150mm. Figure 14 and Figure 15 show the temperature and humidity readings captured shortly after a shower of rain. The signal fluctuations were typical of what would be expected over a day, with the top sensors measuring the highest temperatures and humidity levels.

The second in-road test evaluated the magnetometer's effectiveness and the detection algorithm's response time. Specifically, it examined whether the system could detect an approaching vehicle early enough for the accelerometers to capture the full range of vibrations generated by the vehicle, instead of starting partway through. The length of road on which the installation was performed limited the maximum safe speed to 50 km/h. To

provide maximum variety the tests were therefore conducted for a vehicle approaching the SIRS at speeds 30, 40, and 50km/h. For all three speeds, the magnetometer and the detection algorithm identified vehicles in time, allowing the accelerometers to activate and begin sampling just as needed.

Confident that the SIRS can detect a vehicle in time, the last in-road test aimed at capturing road vibrations as a vehicle moves over the SIRS. The vibrations were captured on 2 layers (in all three directions) at depths of 50 mm and 100 mm, and the vertical road displacement of the road was determined, using the implemented displacement algorithm. The test was conducted with a 2-axle vehicle at three different vehicle speeds, 30km/h, 40km/h, and 50km/h. Examples of the captured vibrations and derived displacement for a vehicle travelling past the SIRS at 40km/h is shown in Figure 16 and Figure 17, respectively. It can be seen that the apparently very noisy acceleration signal is converted into a displacement signal that clearly shows the displacement caused by the consecutive axes, with the top sensor measuring a larger displacement compared to the bottom sensor.

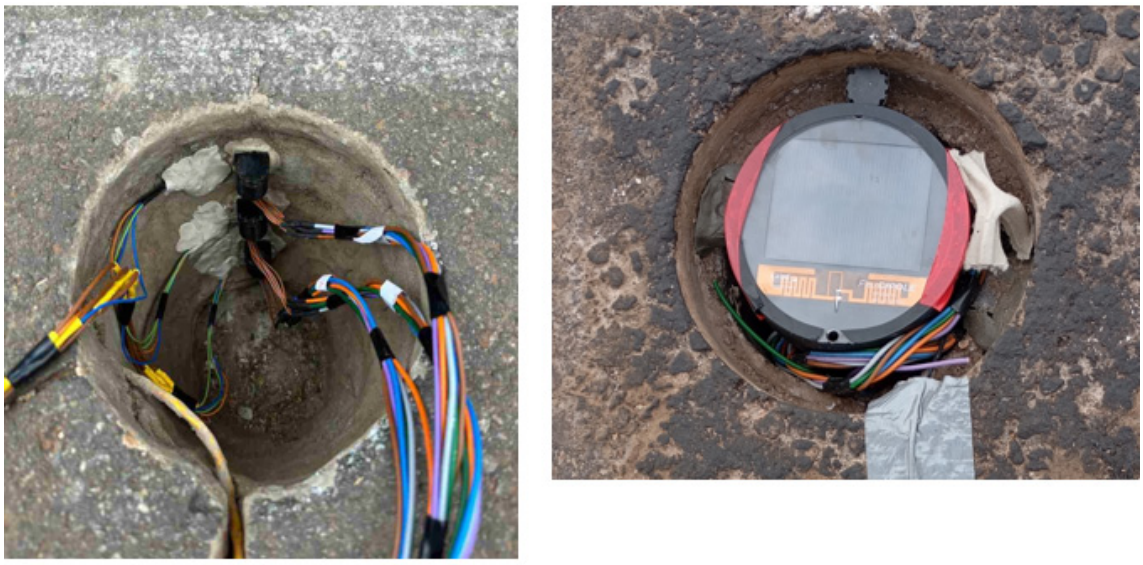

(a) (b)

Figure 13: Sensors and SIRS installed into the core hole on NWU campus

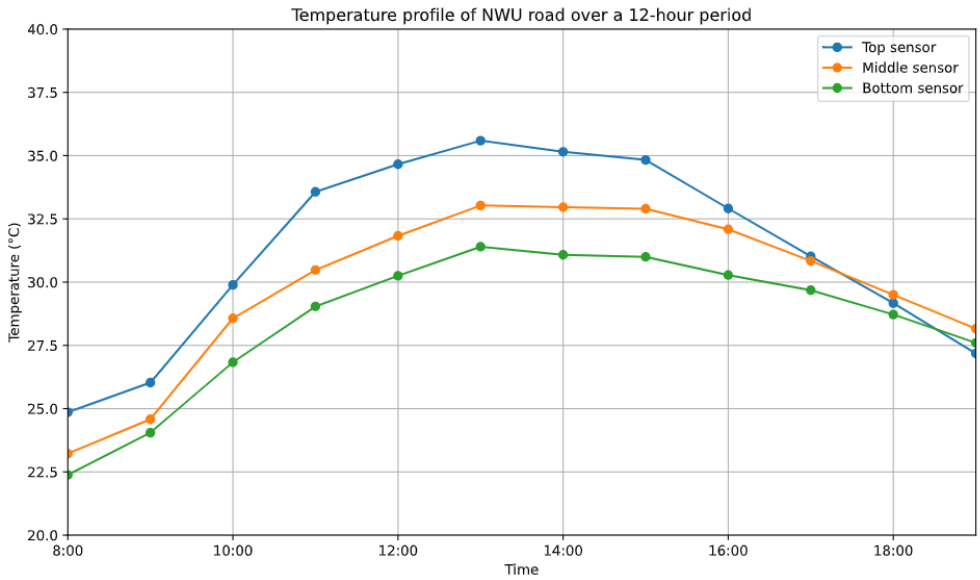

Figure 14: Captured temperature readings inside road

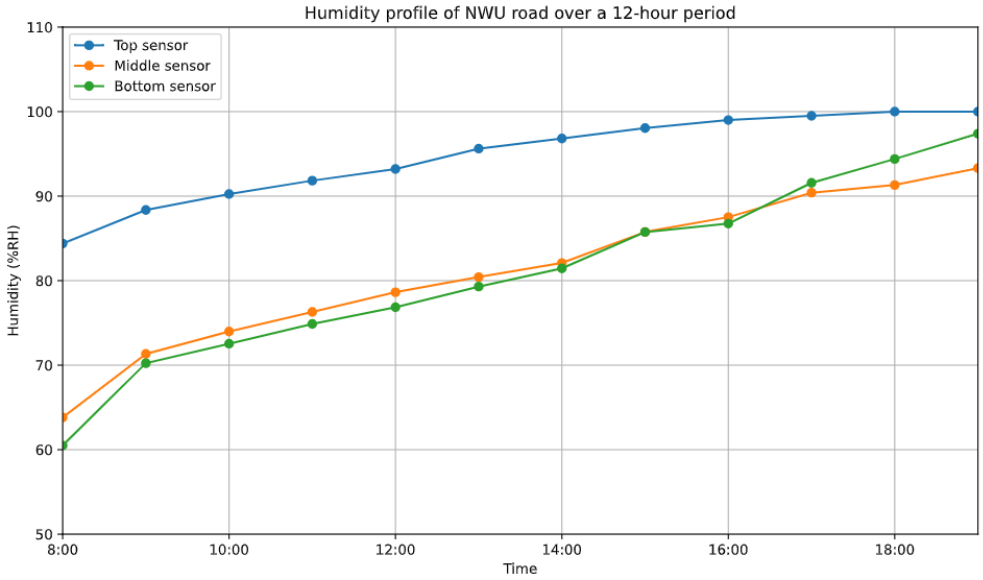

Figure 15: Captured humidity readings inside road

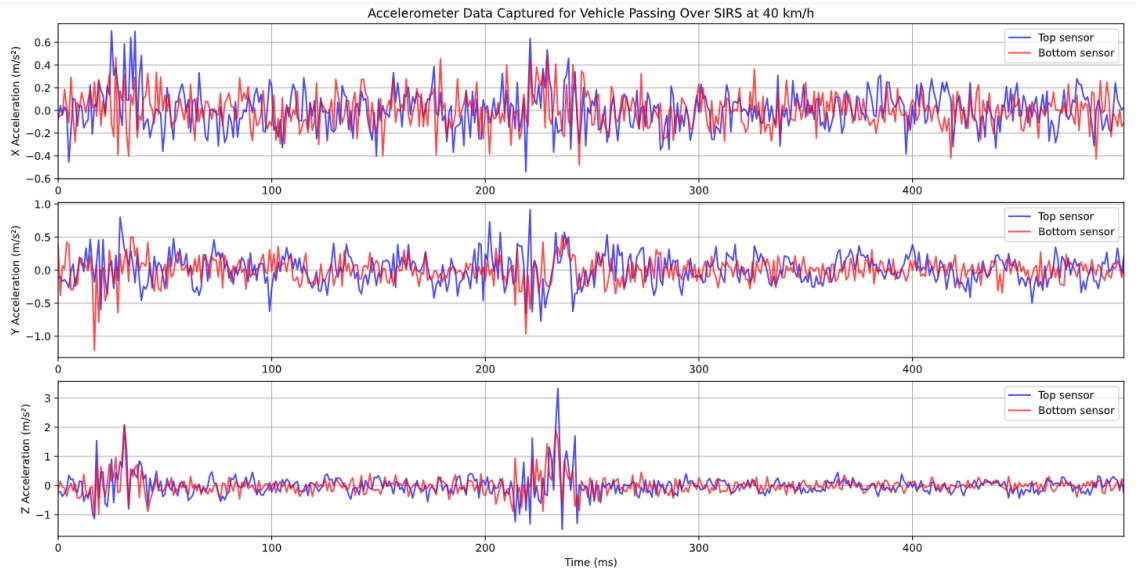

Figure 16: Captured road vibrations for 2-axle vehicle at speed 40km/h

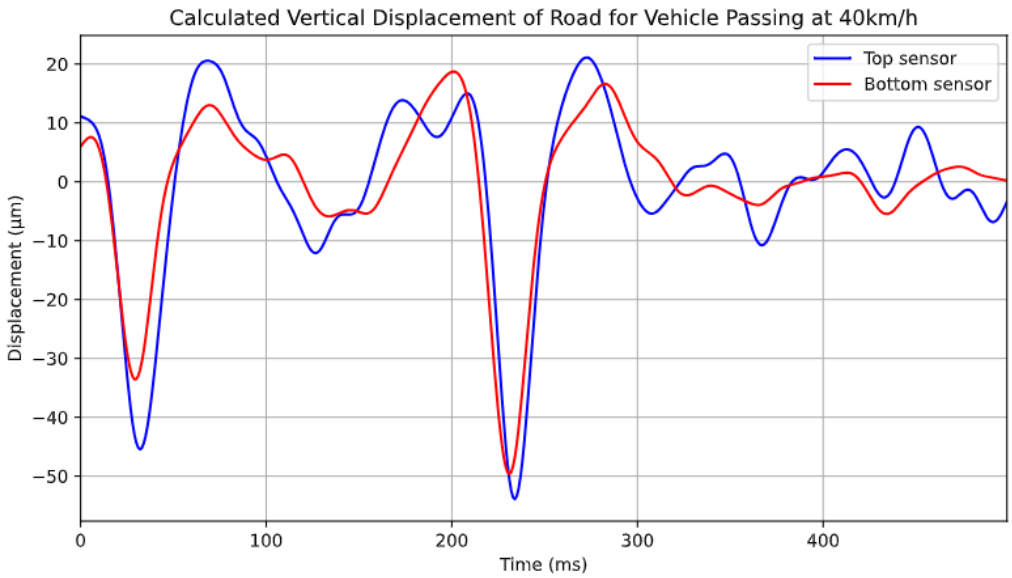

Figure 17: Calculated vertical displacement for 2-axle vehicle at speed 40km/h

5. CONCLUSIONS AND FUTURE WORK

The objective of this work was to develop an improved device for monitoring the condition of road pavements. The requirements included that the device capture temperature, humidity, and vibrations caused by passing vehicles across three different road layers. Additionally, the displacement of the road pavement must be inferred using measured acceleration data, allowing expensive displacement measurement methods to be replaced by low-cost methods. To make the device standalone it must use solar power and a wireless sensors network.

The design of the improved SIRS device was based on technical requirements derived from a detailed literature study. Specialized packagings were developed to enable the installation of the complete device as well as the different sensors inside the road pavement in a manner that ensured that the correct road conditions are measured and that allows retrofitting onto any existing road.

The laboratory tests confirmed that the algorithms used to extract displacement from acceleration produces accurate results across the complete frequency and amplitude ranges of importance for road displacements. The in-road tests confirmed that the packaging of the SIRS and its sensors enables the capturing of actual road conditions in a practical setup. The correct working of the solar panel-based power system and LoRa based sensor network were also successfully demonstrated.

Future work will involve the evaluation of this system on a public highway that is exposed to a variety of vehicle types and high traffic levels. In such a setting the displacements produced by the accelerometers will be compared against the displacements measured by an LVDT device mounted at the same location. The ability of the onboard processor software to extract the displacement values, and the ability of the LoRa network to communicate displacement values for all vehicles triggering the SIRS in real time will also be tested. The system will furthermore be operated over a representative period to determine if the solar panel can sustain the system in all weather conditions and on a 24/7 basis. Lastly the SIRS will be installed in a test road that is subjected to an accelerated life test. Data will be captured from all sensors over the duration of this test and AI (artificial intelligence) methods will be applied to the captured data to determine if both the current state of the road and the remaining useful life can be derived from the collected data.

6. REFERENCES

Alrajhi, A, Roy, K, Qingge, L & Kribs, J. 2023. Detection of Road Condition Defects Using Multiple Sensors and IoT Technology: A Review. *IEEE Open Journal of Intelligent Transportation Systems,* pp (99).

Arraigada, M, Partl, MN, Angelone, SM & Martinez, F. 2009. Evaluation of accelerometers to determine pavement deflections under traffic loads. *Materials and Structures*, 42(6): 779-790.

Bajwa, R, Coleri, E, Rajagopal, R, Varaiya, P & Flores, C. 2020. Pavement performance assessment using a cost-effective wireless accelerometer system. *Computer-Aided Civil and Infrastructure Engineering,* 35(9):1009-1022.

Cafiso, S, Di Graziano, A, Fedele, R, Marchetta, V & Praticò, F. 2021. Sensor-based pavement diagnostic using acoustic signature for moduli estimation. *International Journal of Pavement Research and Technology,* 13(6):573-580.

Ferrero, R, Gandino, F, Hemmatpour, M, Montrucchio, B & Rebaudengo, M. 2016. Exploiting accelerometers to estimate displacement. 5th Mediterranean Conference on Embedded Computing (MECO): 206-210.

Fiorita, A, Fiorita, M & Hoffman, A. 2023. The Development of an IoT In-Road Sensing Device for Pavement Health Monitoring. 2023 IEEE 26th International Conference on Intelligent Transportation Systems (ITSC): 3673-3679.

Kavussi, A, Abbasghorbani, M, Moghadas Nejad, F & Bamdad Ziksari, A. 2017. A new method to determine maintenance and repair activities at network-level pavement management using falling weight deflectometer. *Journal of Civil Engineering and Management,* 23(3):338-346.

Kgamanyane, M & Hartzenberg, T. 2015. The importance of road transport infrastructure development and maintenance in trade facilitation: A South African case, University of Cape Town Faculty of Commerce GSB: Faculty.

Natasha, B, Juliette, B, Pierre, H & Fabien, M. 2020. Alternate Method of Pavement Assessment Using Geophones and Accelerometers for Measuring the Pavement Response, 5:25. Doi: 10.3390/infrastructures5030025.

Rosario, F, Corte, D, Giuseppe, F, Carotenuto, R, Pratico, F & Giammaria, DR. 2017. Sensing road pavement health status through acoustic signals analysis. 13th Conference on Ph.D. Research in Microelectronics and Electronics (PRIME): 165-168.

Ye, Z, Wei, Y, Li, J, Yan, G & Wang, L. A distributed pavement monitoring system based on Internet of Things. *Journal of Traffic and Transportation Engineering* (English Edition), 9(2): 305-317.